

See discussions, stats, and author profiles for this publication at: <https://www.researchgate.net/publication/244404173>

Bonding of Ethers and Alcohols to aCN x Films

ARTICLE *in* LANGMUIR · MARCH 1999

Impact Factor: 4.46 · DOI: 10.1021/la981145a

CITATIONS

33

READS

27

5 AUTHORS, INCLUDING:



Nisha Shukla

Carnegie Mellon University

53 PUBLICATIONS 1,856 CITATIONS

SEE PROFILE



Andrew J. Gellman

Carnegie Mellon University

278 PUBLICATIONS 5,113 CITATIONS

SEE PROFILE



Bruno Marchon

HGST, A Western Digital Company

141 PUBLICATIONS 2,716 CITATIONS

SEE PROFILE

Bonding of Ethers and Alcohols to a-CN_x Films

Kris Paserba, Nisha Shukla, and Andrew J. Gellman*

Department of Chemical Engineering, Carnegie Mellon University,
Pittsburgh, Pennsylvania 15213

Jing Gui and Bruno Marchon†

Seagate Technology, Inc., Fremont, California 94538

Received September 1, 1998. In Final Form: December 1, 1998

The surface chemistry of fluorinated ethers and fluorinated alcohols adsorbed on amorphous nitrogenated carbon (a-CN_x) have been studied as models for the interaction of perfluoropolyalkyl ether (PFPE) lubricants with the surfaces of magnetic data storage media. Temperature-programmed desorption experiments conducted in ultrahigh vacuum using small fluorinated ethers and fluorinated alcohols have measured their desorption energies and have provided insight into the nature of bonding between PFPEs and a-CN_x films. Preliminary results indicate that ether linkages interact with a-CN_x films through electron donation from the oxygen lone pair electrons. In contrast, alcohol end groups show evidence of hydrogen bonding with a-CN_x films. The models derived from this study can aid in the future development of both lubricants and protective overcoats to ensure that the magnetic hard disks display optimal wear resistance and performance.

I. Introduction

Magnetic recording has been the primary technology used to provide long-term data storage in computer systems for over 40 years. After such a long period of development and use, it might be assumed that advances in the field would be minimal. However, progress in the magnetic hard-disk industry today is more rapid than ever. From 1956 to 1991, the annual increase in areal data storage density (number of bits stored per unit area) was approximately 23%.¹ Since 1991, areal density has been increasing at the extraordinary rate of 60% per year. This increase in the storage density has been accompanied by a steady decrease in the flying height of the read-write head over the disk surface. If this current rate is to be maintained or increased, it will be necessary to continue to decrease the separation distance between the read-write head and the magnetic storage medium.

Head-disk contact during operation is unavoidable and occurs during shutdown as the air bearing beneath the head slider is lost as the disk stops spinning. If severe, these high-speed "crashes" can impart high stresses to the disk, potentially damaging the surface and rendering the hard-disk assembly inoperable. Computers today incorporate heads with flying heights of less than 50 nm, and soon it is expected that there will be full contact between the head and the disk surface.² This advancement will place extreme demands on the tribological performance of the protective overcoat and lubricant layer applied to the surface of the storage medium. The key to ensuring optimal wear resistance and performance of the magnetic hard-disk surface is understanding the interactions between the overcoat and lubricant. With such knowledge, it will be possible in the future to tailor lubricants for use with specific overcoats.

Conventional storage devices today guard against "crashes" through the application of a protective overcoat

in the form of a hydrogenated or nitrogenated amorphous carbon (a-CH_x and a-CN_x, respectively) film onto the magnetic storage layer in a thickness of ~100 Å.^{2,3} The chemical bonding of the carbon in these films, which plays a primary role in determining its properties and its interactions with the lubricant, can vary from predominantly sp² to sp³ depending on deposition conditions and hydrogen or nitrogen content. These films also have the desirable properties of high wear resistance, low friction characteristics, and chemical inertness.^{3–5}

In addition to the carbon film, a topical perfluoropolyalkyl ether (PFPE) lubricant film having a thickness of 10–20 Å is applied to further protect the surface of the magnetic storage medium.^{2,6,7} The PFPE molecules are linear polymers with average molecular weights of 2000–4000 amu⁸ and are selected for their low volatility and chemical stability.^{9–14} The PFPE used most commonly in the lubrication of magnetic storage media is Fomblin Zdol, a bifunctional molecule with hydroxyl end groups. This molecule has the general formula HOCH₂CF₂O–(CF₂–CF₂O)_x–(CF₂O)_y–CF₂CH₂OH, where $x/y \approx 2/3$.¹⁵

Interactions between the amorphous carbon overcoat and both the PFPE backbone and functional end groups bond the lubricant to the surface. These interactions are important in minimizing displacement of lubricant during

(3) Teng, E.; Jiaa, C.; Eltoukhy, A. *Surf. Coatings Technol.* **1994**, 68/69, 632.

(4) Bhushan, B.; Kellock, A. J.; Cho, N. H.; Ager, J. W., III *J. Mater. Res.* **1992**, 7 (2), 404.

(5) Kobayashi, A.; Yoshitomi, Yoshihara, O.; Imayoshi, T.; Kinbara, A.; Fumoto, T.; Ueno, M. *Surf. Coatings Technol.* **1995**, 72, 152–156.

(6) O'Connor, T. M.; Back, Y. R.; Jhon, M. S.; Min, B. G.; Yoon, D. Y.; Karis, T. E. *J. Appl. Phys.* **1996**, 79 (8), 5788–5790.

(7) Coffey, K. R.; Raman, V.; Staud, N.; Pocker, D. J. *IEEE Trans. Magn.* **1994**, 30 (6), 4146–4148.

(8) Doerner, M. F.; White, R. L. *MRS Bull.* **1996**, 9, 28–33.

(9) Meyers, J. M.; Gellman, A. J. *Surf. Sci.* **1997**, 372, 171–178.

(10) Lin, J. L.; Bhatia, C. S.; Yates, J. T. *J. Vac. Sci. Technol.* **1995**, A13 (2), 163.

(11) Meyers, J. M.; Street, S. C.; Thompson, S.; Gellman, A. J. *Langmuir* **1996**, 12, 1511–1519.

(12) Monte, E. L.; Kordes, M. E. *J. Vac. Sci. Technol.* **1997**, 15 (3), 1173.

(13) Zehe, M. J.; Faut, O. D. *Tribol. Trans.* **1990**, 33 (4), 634–635.

(14) Walczak, M. M.; Thiel, P. A. *Surf. Sci.* **1989**, 224, 425–450.

* Corresponding author: telephone, 412-268-3848; e-mail, ag4b@andrew.cmu.edu.

† Current address: IBM Almaden Research Labs, San Jose, CA 95120.

(1) Kryder, M. R. *MRS Bull.* **1996**, 9, 17.

(2) Gellman A. J. *Curr. Opin. Colloid Interface Sci.* **1998**, 3 (4), 368.

head-disk contact. In addition, end group interactions with the overcoat and with one another can prevent lubricant spin-off during operation at high rotational speeds (>7200 rpm). However, some mobility of the lubricant is necessary to achieve maximum durability of the hard-disk. The lubricant must be able to flow back into areas of the disk surface depleted of lubricant by repeated head-disk contact. For these reasons, it is important to gain an understanding of the lubricant interactions with amorphous carbon films.

Previous studies indicate that lubricant interactions with amorphous carbon films directly influence the durability and performance of magnetic hard disks. Wang et al.¹⁶ focused on the tribology of the head-disk interface when subjected to contact start-stop (CSS) cycles. The data reported in that study correlate the performance of the magnetic hard-disk with the hydrogen concentration in the a-CH_x overcoat. The CSS durability of magnetic storage media lubricated with Fomblin Zdol was found to improve with increasing hydrogen content in the overcoat. This trend was attributed to changes in lubricant bonding and mobility that occurred as the fraction of sp³ bonding within the overcoat increased. Lee et al.¹⁷ used both a drag test and chemical reactivity test to simulate mechanical and tribochemical wear on a-CH_x films lubricated with several PFPEs. As with Wang et al., improved mechanical durability of the surface was observed with increasing hydrogen incorporation into the film.

The nature of the bonding of fluoroethers to a-CH_x films has been examined in prior work. Cornaglia and Gellman^{18–20} studied the nature of bonding between short-chain ethers and a-CH_x films produced by several manufacturers of data storage media. Desorption energies were determined for hydrocarbon and fluorocarbon ethers adsorbed on the a-CH_x overcoats. In all cases it was found that the desorption energies of the fluorinated ethers were lower than those of the hydrocarbon ethers. This difference in desorption behavior between the hydrocarbon ethers and their fluorinated analogues allowed a model to be proposed for the mechanism of bonding to the carbon films. The model suggests that ethers on a-CH_x films interact through electron donation from the oxygen lone pairs. The same model has been proposed for the bonding of the ethers to several metal surfaces.^{9,11,14,21–23} Within the context of this model, fluorination of the alkyl groups on the ethers is expected to weaken bonding by electron donation to the a-CH_x films, as is observed experimentally.

The focus of the study reported in this work is to understand the nature of the interactions between PFPE lubricants and a-CN_x overcoats at a fundamental molecular level. Although use of actual PFPEs would be ideal, these molecules have very low vapor pressures making them difficult to use under the conditions of this work. Furthermore, they decompose at temperatures above 650

K,²⁴ well below the predicted desorption temperature of ~ 800 K for this class of polymer.¹⁵ This suggests that the PFPE molecules would decompose rather than desorb from a disk surface during heating. Therefore, the approach taken was to study the surface chemistry of short-chain molecules chosen to model the linkages and functional end groups found in PFPEs. Three hydrocarbon ethers and their fluorinated analogues were chosen to represent PFPE linkages. In addition, the hydroxyl end groups present in PFPEs such as Fomblin Zdol were modeled by three alcohols and their fluorinated analogues. Temperature programmed desorption (TPD) studies have allowed estimation of the desorption energy for each model lubricant on a-CN_x films. The observed effects of fluorination on desorption behavior have allowed models to be proposed for the bonding of lubricants adsorbed on a-CN_x films. The results suggest that ethers interact with a-CN_x films through electron donation from oxygen lone pairs while alcohols display evidence of hydrogen bonding.

II. Experimental Section

All experiments were conducted in a stainless steel ultrahigh vacuum (UHV) chamber with a base pressure of 10^{-10} Torr achieved through use of an ion-pump and titanium sublimation pump. The chamber is equipped with two leak valves fitted with stainless steel dosing tubes used to introduce vapor of the model lubricants into the chamber. TPD experiments were performed using an Ametek Dycor MA200M quadrupole mass spectrometer (QMS). This instrument has a mass range of 1–200 amu and is capable of monitoring up to five masses simultaneously as a function of time during a TPD experiment.

Magnetic hard-disks sputtered with an a-CN_x film (20% N₂ atmosphere) were supplied by the Seagate Technology, Inc. Samples ~ 12.5 mm in diameter were machine-punched from the hard-disks for use in the UHV chamber. Two tantalum wires were spot-welded to the edge of the sample disk and mounted to a sample holder at the end of a manipulator capable of x , y , and z translation and 360° rotation. Once mounted, the sample could be cooled to <120 K through mechanical contact with a liquid nitrogen reservoir at the end of the manipulator. In addition, the sample could be heated resistively at a constant rate using a computer to provide proportional-derivative temperature control. The temperature of the sample was measured using a chromel–alumel thermocouple spot-welded to its rear face.

Experiments were conducted using the hard-disk samples as received. During each experiment, the sample was heated to >350 K to induce the desorption of all adsorbed species (including H₂O). No sputtering or cleaning of the sample was performed once in the chamber. Desorption spectra were highly reproducible, indicating that there was no contamination of the surface due to adsorbate decomposition.

Diethyl ether [(CH₃CH₂)₂O, 99+%, dimethoxymethane [CH₃-OCH₂OCH₃, 99%], 1,3-dioxolane [–CH₂OCH₂OCH₂–, 99.5%], ethanol [CH₃CH₂OH, 99.5%], 2-propanol [CH₃CH(OH)CH₃, 99.5%], and perfluoro-*tert*-butyl alcohol [(CF₃)₃COH, 98%] were purchased from Aldrich Chemicals. Perfluorodimethoxymethane [CF₃OCF₂OCF₃, 99.5%] and perfluoro-1,3-dioxolane [–CF₂OCF₂OCF₂–, 99.5%], were supplied by the Wright Patterson AFB. 1,1,1-Trifluoro-2-propanol [CF₃CH(OH)CH₃, 97% min] and 1,1,1,3,3,3-hexafluoro-2-propanol [CF₃CF₂(OH)CF₃, 97% min] were purchased from PCR Chemicals. *tert*-Butyl alcohol [(CH₃)₃COH, 98%] and 2,2,2-trifluoroethanol [CF₃CH₂OH, 99.5%] were purchased from Lancaster Chemicals. Perfluorodiethyl ether [(CF₃CF₂)₂O, 90% min] was purchased from Strem Chemicals. All compounds purchased in liquid form were purified before use through a series of freeze–pump–thaw cycles intended to remove any high vapor pressure contaminants. Compounds purchased in vapor form were used as received.

Within the UHV chamber the sample was positioned adjacent to a stainless steel dosing tube and approximately 2 cm from an

(15) Perry, S. S.; Somorjai, G. A.; Mate, C. M. *Tribol. Lett.* **1995**, *1*, 47–58.

(16) Wang, R.; Meeks, S. W.; White, R. L.; Weresin, W. E. *IEEE Trans. Magn.* **1995**, *31* (6), 2919–2921.

(17) Lee, J. K.; Smallen, M.; Enguero, J.; Lee, H. J.; Chao, A. *IEEE Trans. Magn.* **1993**, *29* (1), 276–281.

(18) Cornaglia, L.; Gellman, A. J. *J. Vac. Sci. Technol.* **1997**, *15* (5), 1–11.

(19) Cornaglia, L.; Gellman, A. J.; Howe, S.; Nadimpalli S. *Tribology of Contact/Near Contact Recording for Ultrahigh-Density Magnetic Storage*; Bhatia, S.; Menon, A. K., Eds.; 1996; pp 38–44.

(20) Cornaglia, L.; Gellman, A. J. *Adv. Info. Stor. Sys.* **1998**, *8*, 57.

(21) Meyers, J. M.; Gellman, A. J. *Tribol. Lett.* **1996**, *2*, 47.

(22) Walczak, M. M.; Leavitt, P. K.; Thiel, P. A. *J. Am. Chem. Soc.* **1987**, *109*, 5621.

(23) Walczak, M. M.; Leavitt, P. K.; Thiel, P. A. *Trib. Trans.* **1990**, *33*, 557.

(24) Helmick, L. S.; Jones Jr., W. R. *NASA Tech. Memo.* **1990**, 102493.

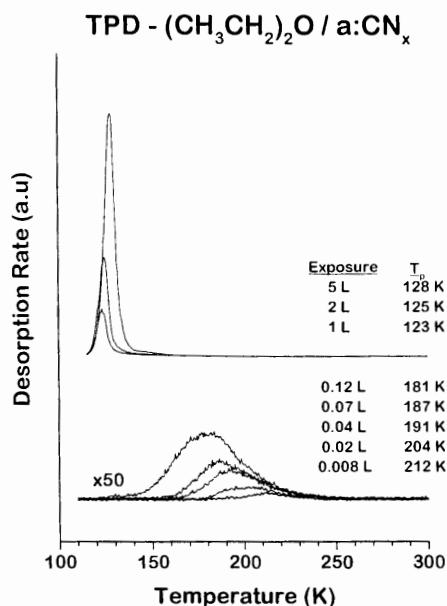


Figure 1. TPD spectra of diethyl ether [(CH₃CH₂)₂O] obtained as a function of exposure following adsorption on the a-CN_x surface at 100 K. The spectra were generated by monitoring mass 59 (CH₃CH₂OCH₂⁺). The heating rate was 2 K/s.

aperture leading to the QMS. TPD studies were conducted by cooling the disk sample in UHV to <120 K and exposing its surface to vapor of the model lubricants at pressures ranging from 10⁻⁹ to 2.5 × 10⁻⁸ Torr for periods of 10–200 s. The exposures are reported in units of langmuirs (1 langmuir = 10⁻⁶ Torr·s) without correction for ion-gauge sensitivity. Following adsorption of the compounds on the a-CN_x surface, the sample was heated at a constant rate of 2 K/s to temperatures in the range 370–450 K. During heating, the QMS was used to monitor the desorption of the adsorbed species and any decomposition products if present. In all cases, adsorption of the model lubricant was both molecular and reversible with no indication of decomposition.

III. Results

Desorption of Diethyl Ether and Perfluorodiethyl Ether. The nature of the interaction of ether backbone linkages in PFPEs with a-CN_x surfaces has been quantified by studying the adsorption of small hydrocarbon and fluorocarbon ethers. The desorption energies of the ethers on a-CN_x films have been determined using TPD. Figure 1 shows the TPD spectra of diethyl ether [(CH₃CH₂)₂O] as a function of exposure to the a-CN_x surface at 100 K. The spectra were generated by using the QMS to monitor the signal at *m/q* = 59 (CH₃CH₂OCH₂⁺), the most intense ion in the fragmentation pattern, during heating. Several additional mass-to-charge ratios were monitored including *m/q* = 2 (H₂⁺), *m/q* = 29 (CH₃CH₂⁺), *m/q* = 31 (CH₂OH⁺), and *m/q* = 45 (CH₃CH₂O⁺) to detect the desorption of any decomposition products if present. No decomposition was observed for diethyl ether or any of the hydrocarbon ethers studied.

The dependence of the desorption spectra on ether coverage is very similar for all the ethers studied. At the lowest coverage diethyl ether desorbs over a broad temperature range and achieves a maximum rate of desorption at 212 K, as shown in Figure 1. As the exposure is increased, the desorption peak intensifies and shifts to lower temperatures until the monolayer is saturated. Following monolayer saturation, a desorption feature grows in at ~125 K that does not saturate with increasing coverage and displays zero-order kinetics indicative of the bulk sublimation of multilayers. This temperature is consistent with the multilayer desorption temperatures

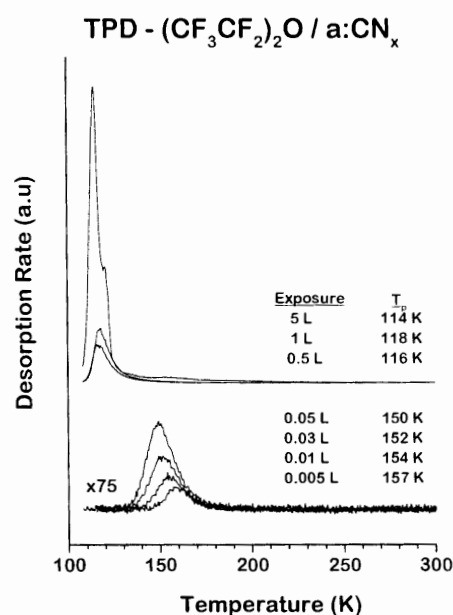


Figure 2. TPD spectra of perfluorodiethyl ether [(CF₃CF₂)₂O] obtained as a function of exposure following adsorption on the a-CN_x surface at 100 K. The spectra were generated by monitoring mass 69 (CF₃⁺). The heating rate was 2 K/s.

found for diethyl ether adsorbed on a-CH_x films (123 K),² Cu(100) (135 K),²⁵ Pt(111) (129 K),²⁶ and Ru(0001) (130 K).¹⁴

By comparing the desorption characteristics of small hydrocarbon and fluorocarbon ethers, it has been possible to gain some insight into the nature of the interaction of the PFPE backbone with the a-CN_x surface. Figure 2 shows TPD spectra of perfluorodiethyl ether [(CF₃CF₂)₂O] following varying exposure to the a-CN_x surface at 100 K. The spectra were generated by using the QMS to monitor the signal at *m/q* = 69 (CF₃⁺) during heating. Several additional mass-to-charge ratios were monitored including *m/q* = 50 (CF₂⁺) and *m/q* = 31 (CF⁺) to detect the desorption of any decomposition products if present. No decomposition was observed for perfluorodiethyl ether or any of the fluorocarbon ethers studied. The characteristics and behavior of the spectra are qualitatively similar to those illustrated in Figure 1 for diethyl ether. At lowest coverage the adsorbed perfluorodiethyl ether desorbs with a maximum rate at 157 K, substantially lower than that observed for diethyl ether (212 K). In addition, the width of the submonolayer desorption peaks for perfluorodiethyl ether desorption are narrower than those of diethyl ether. The multilayer desorption temperature was ~118 K and is consistent with the results obtained for multilayer perfluorodiethyl ether desorption from a-CH_x films (113 K),² Al (110) (111 K),⁹ Cu(111) (122 K),¹¹ and ZrO₂ films (125 K).²⁷ Figure 2 illustrates qualitatively the desorption behavior observed for all the fluoroethers used in this study.

Desorption of Ethanol and 2,2,2-Trifluoroethanol. Alcohols were chosen to model the hydroxyl end groups present in PFPEs such as Fomblin Zdol. As with the ethers, TPD spectra were used to estimate interaction strengths of various alcohols adsorbed on a-CN_x films. Figure 3 shows TPD spectra obtained as a function of ethanol (CH₃CH₂-OH) exposure to the a-CN_x surface at 115 K. The spectra were generated by using the QMS to monitor *m/q* = 31

(25) Sexton, B. A.; Hughes, A. E. *Surf. Sci.* **1984**, *140*, 227–248.

(26) Rendulic, K. D.; Sexton, B. A. *J. Catal.* **1982**, *78*, 126–135.

(27) Maurice, V.; Takeuchi, K.; Salmeron, M.; Somorjai, G. A. *Surf. Sci.* **1991**, *250*, 99–111.

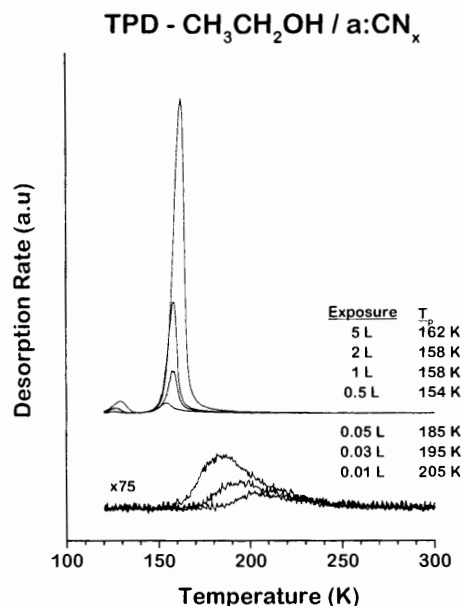


Figure 3. TPD spectra of ethanol ($\text{CH}_3\text{CH}_2\text{OH}$) obtained as a function of exposure following adsorption on the a- CN_x surface at 115 K. The spectra were generated by monitoring mass 31 (CH_2OH^+). The heating rate was 2 K/s.

(CH_2OH^+) during heating. Additional mass-to-charge ratios were monitored including $m/q = 29$ (CHO^+) and $m/q = 45$ ($\text{CH}_3\text{CH}_2\text{O}^+$) to detect the desorption of any decomposition products if present. No decomposition was observed for ethanol or any of the hydrocarbon alcohols studied. At lowest coverage the adsorbed ethanol desorbs with a maximum rate at 205 K. The temperature observed for multilayer desorption was ~ 158 K and is consistent with results reported for multilayer ethanol desorption from Cu(100) (155 K),²⁶ ZrO_2 (160 K),²⁷ and Ag(110) (155 K).²⁸ Figure 3 illustrates qualitatively the desorption spectra of all the hydrocarbon alcohols used in this study.

As with the ethers, the effects of fluorination on desorption behavior of alcohols were studied in order to gain insight into the nature of the interaction of PFPE hydroxyl groups with the a- CN_x film. Figure 4 shows the TPD spectra of 2,2,2-trifluoroethanol ($\text{CF}_3\text{CH}_2\text{OH}$) following various exposures to the a- CN_x surface at 115 K. The spectra were generated by using the QMS to monitor the signal at $m/q = 31$ (CH_2OH^+) during heating. The mass-to-charge ratio of $m/q = 69$ (CF_3^+) was monitored also to verify that decomposition products were not present. No decomposition of 2,2,2-trifluoroethanol or any of the fluorocarbon alcohols studied was observed. Upon fluorination of the methyl group of ethanol, the adsorbed monolayer at lowest coverage desorbs with a maximum rate at 220 K. This represents an increase of 15 K over the low coverage desorption temperature of ethanol. The sublimation of multilayers of 2,2,2-trifluoroethanol occurs at 159 K. This observation is consistent with the multilayer desorption temperatures found for 2,2,2-trifluoroethanol adsorbed on Cu(111) (165 K)²⁹ and ZrO_2 (155 K).²⁷ Figure 4 illustrates qualitatively the desorption spectra of all the fluorinated alcohols used in this study.

Care is needed in identifying the low coverage desorption temperatures and desorption energies (ΔE_d) of the alcohols because the desorption peaks are broad and the difference between peak temperatures upon fluorination is small. To properly compare the interaction strengths of the two

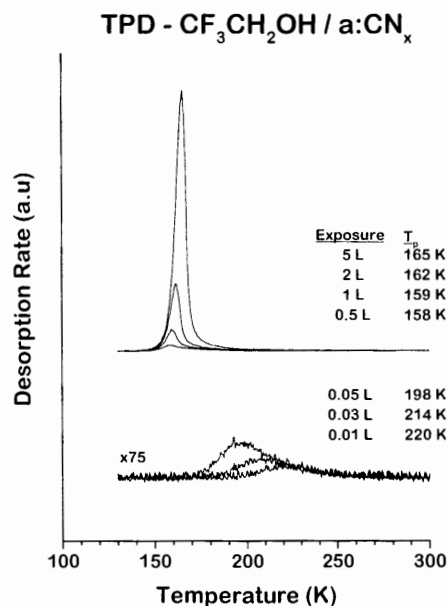


Figure 4. TPD spectra of 2,2,2-trifluoroethanol ($\text{CF}_3\text{CH}_2\text{OH}$) obtained as a function of exposure following adsorption on the a- CN_x surface at 115 K. The spectra were generated by monitoring mass 31 (CH_2OH^+). The heating rate was 2 K/s.

Alcohol Desorption Energy versus Coverage

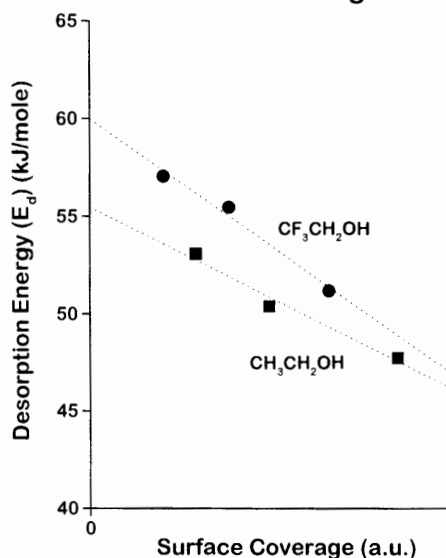


Figure 5. Desorption energies as a function of coverage for ethanol and 2,2,2-trifluoroethanol adsorbed on the a- CN_x overcoat. To accurately compare results between molecules, a linear fit has been used to estimate the desorption energy (ΔE_d^0) in the limit of zero surface coverage.

alcohols when adsorbed on a- CN_x films, it was necessary to determine the desorption energies as a function of exposure for each and extrapolate to the limit of zero surface coverage. Figure 5 shows a plot of desorption energy as a function of exposure for ethanol and 2,2,2-trifluoroethanol (the analysis of desorption temperature to estimate desorption energy is discussed below). A straight line has been fit to each data set that allows estimation of the desorption energy in the limit of zero surface coverage, denoted ΔE_d^0 . As illustrated in Figure 5, ΔE_d^0 of 2,2,2-trifluoroethanol is approximately 5 kJ/mol greater than ΔE_d^0 of ethanol. The fundamentally important observation of this work is that while the interaction of the ethers with a- CN_x is weakened by

(28) Zhang, R.; Gellman, A. J. *J. Phys. Chem.* **1991**, *95*, 7433–7437.

(29) McFadden, C.; Gellman, A. J. *Langmuir* **1995**, *11*, 273–280.

fluorination, the interaction of the alcohols with a-CN_x is strengthened by fluorination. This indicates that there is a significant difference in the nature of their interactions with the surface of the a-CN_x film.

IV. Discussion

Desorption Energies of Model Lubricants on a-CN_x Overcoats. The desorption energies, ΔE_d , of the ethers and alcohols from the a-CN_x surface have been estimated using Redhead's equation³⁰ with the assumption that monolayer desorption occurs with first-order desorption kinetics

$$\frac{\Delta E_d}{RT_p^2} = \frac{\nu}{\beta} \exp\left(-\frac{\Delta E_d}{RT_p}\right)$$

where ν is a preexponential factor (assumed in this case to be $\sim 10^{13} \text{ s}^{-1}$), β is the heating rate, R is the universal gas constant, and T_p is the desorption peak temperature. This is consistent with analyses of desorption on metal surfaces such as Cu(111).^{11,21} A careful study of the desorption kinetics of the fluoroethers on that surface fit the data to first-order desorption profiles with little interaction between adsorbed molecules. Those interactions that were observed were attractive, and at highest coverage their magnitude was roughly 5% that of the metal adsorbate interaction strength. On the basis of this work it is reasonable to suggest that a first-order rate expression is appropriate for desorption from the a-CN_x surface.

It is important to note that in this work we have focused on the desorption energies of the ethers and alcohols at low coverage. The surfaces of the a-CN_x films are undoubtedly very heterogeneous, and it is this heterogeneity which must contribute to the width of the desorption peaks observed as the adsorbate coverage is increased. By comparison the monolayer desorption features for ethers on single-crystal Cu(111) surfaces are very narrow and are consistent with simple first-order desorption kinetics with very little interaction between the adsorbed fluoroethers.¹¹ Thus the assumption of first-order desorption kinetics seems reasonable in this case, and the width of the desorption features is attributed to inhomogeneity in the a-CN_x surface. This heterogeneity has also been observed on the a-CH_x surface.¹⁸

Given the complexity and apparent heterogeneity of the a-CN_x surface, it is only meaningful to compare desorption energies in the limit of low coverage (ΔE_d^0) and anything more than a simple Redhead analysis of the data was felt to be unwarranted. Figures 6 and 7 give values of ΔE_d^0 for the ethers and alcohols, respectively, when adsorbed on a-CN_x films. Figure 6 shows that ΔE_d^0 decreases by 12–17 kJ/mol when fluorine is substituted into the ethers. In direct contrast, ΔE_d^0 for the alcohols increases by 4–10 kJ/mol upon fluorination as shown in Figure 7. These trends have allowed models to be proposed for bonding of both the ethers and alcohols to the a-CN_x films. The interaction of the ethers with a-CN_x films will be addressed first, followed by a discussion of the model proposed for the interaction of the alcohols with the a-CN_x surface.

Interaction of Ethers with a-CN_x Films. The primary observation made during our study of the desorption of the ethers has been that the desorption energies of the fluoroethers on a-CN_x films are 12–17 kJ/mol lower than those of their hydrocarbon analogues. This leads to the suggestion that the bonding of ethers to a-CN_x films is

Desorption Energies Ethers / a-CN_x

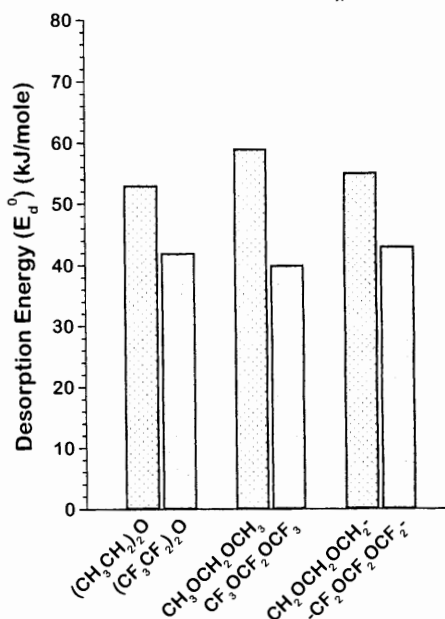


Figure 6. Desorption energies of the ethers adsorbed on a-CN_x overcoats. All reported desorption energies are in the limit of zero surface coverage. These numbers clearly indicate that fluorination decreases ΔE_d^0 for the ethers.

Desorption Energies Alcohols / a-CN_x

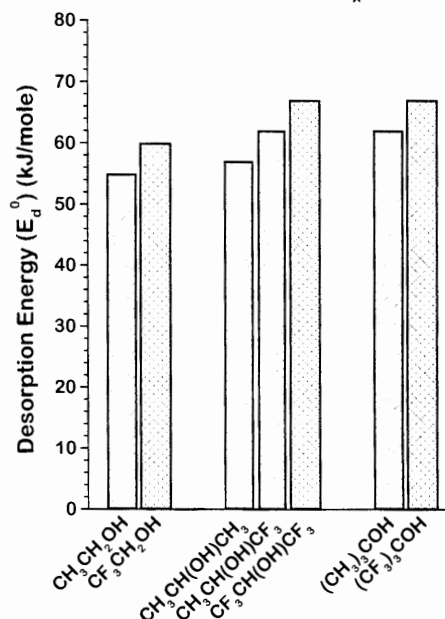


Figure 7. Desorption energies of the alcohols adsorbed on a-CN_x overcoats. All reported desorption energies are in the limit of zero surface coverage. These numbers clearly indicate that fluorination increases ΔE_d^0 for the alcohols.

due to donation of electron density from the oxygen lone pairs. Figure 8 depicts a model for the interactions of diethyl ether and perfluorodiethyl ether with a-CN_x overcoats and is consistent with the observed behavior of all the ethers studied. The dominant interaction of the ethers with a-CN_x films involves formation of a dative bond by way of electron donation from oxygen lone pairs to the overcoat. While this interaction should not be

(30) Redhead, P. A. *Vacuum* **1962**, *12*, 203–211.

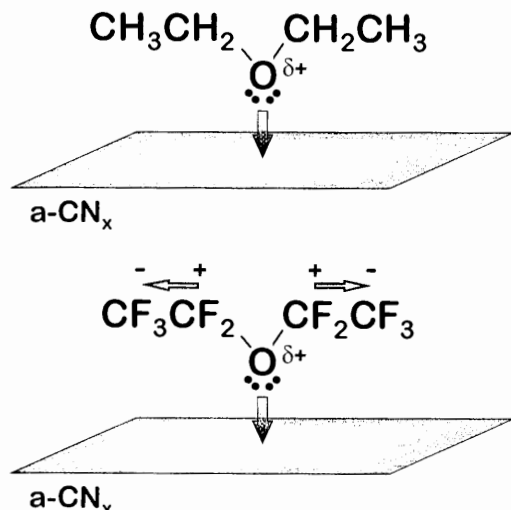


Figure 8. Proposed models for the interactions of diethyl ether and perfluorodiethyl ether with the $a\text{-CN}_x$ surface. A dative bond is formed via electron donation from oxygen lone pairs to the amorphous film. The increased magnitude of the local dipoles on the fluorinated ethyl groups in perfluorodiethyl ether results in a destabilization of the partial positive charge induced on oxygen by electron donation. This results in a decrease in ΔE_d^0 upon fluorinating the ethers.

thought of as covalent bonding, its contribution to the desorption energy of the ethers on $a\text{-CN}_x$ films is significant.

Substitution of fluorine into the hydrocarbon ethers decreases the strength of interaction with the $a\text{-CN}_x$ film. The physical basis or concepts used to understand the effects of fluorine substitution (or other substitutions) on the properties of molecules are described in the literature of physical organic chemistry.³¹ Within the context of the model suggested for the bonding of the ethers to the $a\text{-CN}_x$ film, the donation of electrons from the oxygen atom renders it electron deficient with respect to the desorbed (gas phase) state. This is depicted in Figure 8 as a $\delta+$ on the oxygen atom. It is important to realize that this is not intended to represent the absolute charge on the oxygen atom but rather the change in the charge density as a result of adsorption from the gas phase. The inductive effect of fluorine creates local dipole moments on each CF_3CF_2- group as shown in Figure 8. These dipole moments are much greater than those of the CH_3CH_2- groups on diethyl ether, and in the fluoroether they electrostatically destabilize (increase potential energy) the adsorbed species. This is a result of the repulsive electrostatic interaction between the dipole moments on the CF_3CF_2- groups and the oxygen atom, which is electron deficient due to electron donation to the surface on adsorption. This effect leads to a decrease in the strength of the dative bond and is the primary reason for the observed decrease in ΔE_d^0 of the fluoroethers with respect to their hydrocarbon analogues.

Previous studies have indicated that ethers interact with $a\text{-CH}_x$ films in the same manner as described for the $a\text{-CN}_x$ films. Cornaglia and Gellman¹⁸ investigated the surface chemistry of fluoroethers adsorbed on $a\text{-CH}_x$ films in UHV environments using TPD. In all cases the desorption energies of the fluoroethers were 6–15 kJ/mol lower than those of their hydrocarbon analogues. Maurice et al.²⁷ studied the bonding of both diethyl ether and perfluorodiethyl ether to zirconium oxide (ZrO_2) thin films in UHV. The saturated monolayer of perfluorodiethyl ether

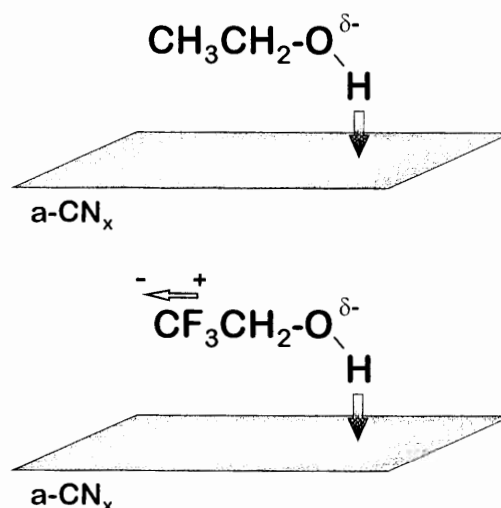


Figure 9. Proposed models for the interaction of ethanol and 2,2,2-trifluoroethanol with the $a\text{-CN}_x$ surface. Both molecules donate a proton to the amorphous film thereby forming a hydrogen bond. The increased magnitude of the local dipole on the fluorinated ethyl group in 2,2,2-trifluoroethanol results in a stabilization of the partial negative charge induced on oxygen by proton donation. This results in an increase in ΔE_d^0 upon fluorinating the alcohols.

adsorbed on ZrO_2 was found to have a desorption energy that is 19 kJ/mol less than that of diethyl ether. It was concluded that the ethers interacted with ZrO_2 films through electron donation from oxygen lone pairs. The observed trend in the desorption energies of the two ethers was attributed to the suppression of oxygen lone pair donation by highly electronegative fluorine.

As a final point of comparison, a recent study has calculated the proton affinities (PA) of dimethyl ether (CH_3OCH_3) and perfluorodimethyl ether (CF_3OCF_3).³² These calculations reveal structures in which the proton is shown to interact with the oxygen atom of the ether. The PA of dimethyl ether is calculated to be 810 kJ/mol, which is in very close agreement with the experimental number of 804 kJ/mol. Fluorination reduces the PA to 602 kJ/mol in perfluorodimethyl ether. The sign of the effect is the same as that observed in our study of ether interaction with the $a\text{-CN}_x$ surface although the magnitude of the interaction with a bare proton is much greater. However, the relative effects of fluorination are very similar in the two systems. Fluorination reduces the PA of dimethyl ether by about 25% and the ΔE_d^0 of the ethers on $a\text{-CN}_x$ by about 25%.

Interactions of Alcohols with $a\text{-CN}_x$ Films. The primary observation made in our study of the adsorption of alcohols on the $a\text{-CN}_x$ surface is that fluorination of the alcohols results in an increase in the desorption energy. This is in direct contrast to the observation made for the ethers. The acidic nature of alcohols makes them primary candidates for participating in proton donation or hydrogen bonding. Figure 9 illustrates the proposed bonding mechanisms for ethanol and 2,2,2-trifluoroethanol adsorbed on the $a\text{-CN}_x$ surface and is representative of the expected behavior of all alcohols studied. Interactions between alkyl groups and the $a\text{-CN}_x$ surface tend to be weak. The primary interaction between ethanol and the $a\text{-CN}_x$ surface involves donation of a proton to the carbon film. In essence, the alcohols act as simple proton donors with properties much like Brønsted acids except that they are not completely deprotonated. This renders the oxygen

(31) Taft, R. W.; Topsom, R. D. *Prog. Phys. Org. Chem.* **1987**, 1.

(32) Orgel, V. B.; Ball, D. W.; Zehe, M. J. *J. Mol. Struct. (THEOCHEM)* **1997**, 417, 195–202.

atom electron rich with respect to its desorbed state (gas phase). Fluorination of the alcohol to produce 2,2,2-trifluoroethanol introduces a dipole moment into the CF₃-CH₂- groups that is much greater than the dipole moment of the CH₃CH₂- group in ethanol. This dipole moment energetically stabilizes (lowers potential energy) the adsorbed species through electrostatic interaction with the electron-rich oxygen atom, thereby increasing ΔE_d^0 . Although the model proposed for bonding of ethanol with a-CN_x is a reasonable interpretation of the results, the nature of the proton acceptor in the film is unclear. It is important to note that exposure to air oxidizes these films to form partially oxidized carbonaceous species such as alcohol groups, acids, and esters on the surface of the carbon film. The oxygen in the film could serve as the proton acceptor, as could the nitrogen. These questions remain unanswered at this point.

There are several systems in which fluorination of alcohols exhibits similar results to those observed in this study. For example, it is well-documented that fluorinated alcohols are stronger acids having higher pK_a values than their hydrocarbon analogues.³³ The effects of fluorination on alcohol interaction with a-CN_x can be compared with the results of a computational investigation of the hydrogen bonding of alcohols with water.³⁴ The alcohol-water potentials were derived for 2-propanol, 1,1,1-trifluoro-2-propanol, and 1,1,1,3,3,3-hexafluoro-2-propanol. It is clear from the structures determined for the alcohol-water complexes that hydrogen bonding occurs through proton donation from the alcohol to water. Fluorination of the alcohol increases the strength of the hydrogen bond: 25.28 kJ/mol (2-propanol), 34.87 kJ/mol (1,1,1-trifluoro-2-propanol), and 36.94 kJ/mol (1,1,1,3,3,3-hexafluoro-2-propanol). This effect is of the same magnitude and same sign as the effect of fluorination on the ΔE_d^0 of the 2-propanols on the a-CN_x films.

In another study of hydrogen bonding Ladika et al.³⁵ investigated the interactions between monosubstituted benzenes and ethanol, 2,2,2-trifluoroethanol, 2-propanol, and 1,1,1,3,3,3-hexafluoro-2-propanol using ¹H NMR shifts of the hydroxyl hydrogen in the complex. Although bond strengths between hydroxyl hydrogen and the aromatic compounds were not determined quantitatively, the observed chemical shifts indicate that the hydrogen bond interaction becomes stronger with increasing fluorination.

Implications for Hard-Disk Technology. Protection of the surfaces of magnetic storage media is provided by a combination of a sputtered amorphous carbon film coated with a PFPE lubricant such as Fomblin Zdol. It has been established that the performance of this system depends not only on the characteristics of the lubricant but also

on the characteristics of the carbon overcoat.^{16,17} The two cannot be considered independently. In this investigation we have demonstrated that the interactions between the ether linkages of the PFPE and a-CN_x films differ in nature from the interaction of the hydroxyl end groups with a-CN_x. The implication of this is that changes made in the hydrogen or nitrogen concentrations or other properties of the carbon films will have different effects on the interactions of PFPE backbone (ether) and end groups (hydroxyl).

The amorphous nature of the carbon films conventionally used in the manufacturing of hard-disks dictates that there will be a variety of surface sites available for lubricant bonding. Dangling bonds present in a-C films would probably participate as binding sites for adsorbed molecules. In addition, oxygen reacts with the amorphous carbon surface to produce functional groups that can also serve as adsorption sites for lubricant molecules. The TPD spectra in Figures 1–4 show direct evidence that a broad distribution of binding sites exists on the a-CN_x surface. The width of the peaks in the monolayer regime ($\Delta T \sim 55$ –100 K) clearly indicates that adsorption occurs on many different sites, each with a characteristic adsorption energy. These are much broader than the desorption features observed on a Cu(111) surface ($\Delta T \sim 10$ K) where it has been shown that the desorption process is first order and that the intermolecular interactions between fluoroethers that might be responsible for the peak broadening are in fact quite small. The distribution in the desorption energies that is implied by the coverage dependence of our desorption spectra must also influence the interactions of PFPE lubricants with amorphous carbon surfaces.

V. Conclusions

The use of small fluorinated ethers and fluorinated alcohols has provided insight into the interactions between perfluoropolyalkyl ether lubricants and a-CN_x films. These results indicate that ether linkages of PFPEs interact with a-CN_x films primarily through electron donation from oxygen lone pairs. In the case of ethers the interaction strength decreases by ~25% as a result of fluorination. In contrast, the hydroxyl end groups of alcohols show evidence of hydrogen bonding with a-CN_x surfaces. The hydrogen bond between the hydroxyl proton and the a-CN_x surface increases in strength by ~10% as a result of fluorination. At this point these models appear to be general in the sense that for the ethers they apply both to a-CH_x and to a-CN_x. The models presented in this paper may serve as useful guidelines to understanding the different interactions of functional groups present in PFPE lubricants with a-CN_x overcoats.

Acknowledgment. Support for this work is gratefully acknowledged from the Seagate Technology, Inc., and from the NSF under Grant Number ECD-8907068.

LA981145A

(33) Banks, R. E. *Organofluorine Chemistry: Principles and Commercial Applications*; Plenum Press: New York, 1994.

(34) Kinugawa, K.; Nakanishi, K. *J. Chem. Phys.* **1988**, *89* (9), 5834–5842.

(35) Ladika, M.; Jursic, B.; Sunko, D. E. *Spectrochim. Acta* **1986**, *42A* (12), 1397–1400.